Atmospheric Environment Pergamon Press 1971. Vol. 5, pp. 527–540. Printed in Great Britain.

SIZE DISTRIBUTION OF ATMOSPHERIC GIANT PARTICLES

KENNETH E. NOLL and MICHAEL J. PILAT

Department of Civil Engineering, University of Washington, Seattle, Washington 98105, U.S.A.

(*First received* 12 *February* 1970 *and in final form* 22 *April* 1970)

Abstract—The size distribution of atmospheric giant particles in the range 5–100 μm radius was measured at three locations in Washington State using a rotary inertial impactor. The size distribution was continuous at the different locations. A significant change in the slope of the $dN/d\log r$ vs. r plot of the size distribution generally occurred between 30 and 40 μm radius. The slope B ($dN/d\log r = Ar^{-B}$) in the 5–25 μm radius range averaged 2.3 while in the 40 to 100 μm radius range B averaged 6.7.

A complete atmospheric aerosol size distribution for the 0.01–100 μm radius range was obtained by combining thermal precipitator (0.01–1 μm) and inertial impaction (5–100 μm) data. It followed from the calculation of the atmospheric aerosol mass distribution (assuming spherical particles of unit density) that approximately 20 per cent of the total mass was in particles of less than 1 μm radius, 35 per cent in the 1–10 μm range, 45 per cent in the 10–50 μm range, and less than 1 per cent in the greater than 50 μm radius range.

1. INTRODUCTION

(a) *Significance of atmospheric giant particles*

Giant particles (diameter greater than 1 μm) are an important part of the atmospheric aerosol which in general ranges from 0.01 to 100 μm in radius. Giant particles are responsible for the fallout of suspended particulate matter (measured with fallout jars) of which the detrimental effects include soiling and the contamination of open water supplies was reported by JOHNSON *et al.* (1966). The surface of giant particles provide sorption and nucleation sites (PILAT, 1968; TWOMEY, 1954) and may act as condensation nuclei in the precipitation process. In spite of the importance of giant atmospheric particles, little is known about their size distribution or its variation with changes in location and weather conditions. Routine monitoring of the particulate air pollutant concentration includes only the mass concentration and this is not adequate to characterize the atmospheric aerosol size distribution.

(b) *Literature review*

The particulate pollution of an urban atmosphere is the result of complicated processes, depending on the size distribution of particles emitted into the atmosphere and atmospheric processes (coagulation, sedimentation, rainout, chemical reactions, etc.). JUNGE (1955) observed a systematic decrease in concentration with size from a peak concentration near 0.01 μm. This decrease can be approximated by $dN/d\log r = Ar^{-B}$ where B is the slope of the distribution ($dN/d\log r$ vs. r) on log–log paper. Consideration of aerosol mechanics led FRIEDLANDER and WANG (1966) to develop a similar mathematical form to describe the distribution of particle size as a function of aerosol concentration.

The amount of published information on the size distribution of giant particles in the atmosphere is small. However, JAENICKE and JUNGE (1967), OKITA (1955), and WOODCOCK (1953) have provided information which can be compared to the data

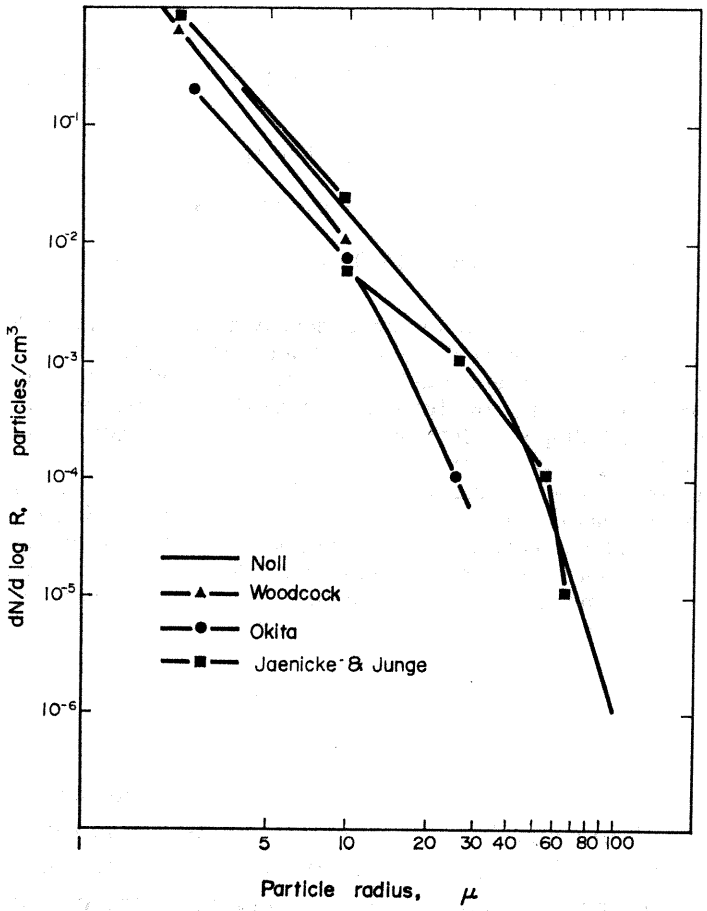

FIG. 1. A comparison of atmospheric giant aerosol size distributions.

collected in this investigation and their data are shown in FIG. 1. Jaenicke and Junge sampled giant particles with a propeller type inertial impactor and collected particles larger than 10 μm radius. They concluded that the coarse aerosol was a very regular component of the air, and its size distribution was continuous with the distribution between 0.1 and 10 μm. Okita used a sedimentation technique and also sampled particles on web threads to determine the size distribution of particles in the heavily polluted area of Asahigawa, Japan. The exponent, B, differed for different particle size ranges as follows:

0.5–10 μm	$dn/d\log r = Ar^{-2.6}$
10–40 μm	$dn/d\log r = Ar^{-3.7}$
Greater than 40	$dn/d\log r = Ar^{-6.5}$

WOODCOCK (1949, 1952, 1953) and MOORE and MASON (1954) conducted studies of large and giant aerosols over the ocean. Both used impactor techniques with glass slides mounted on the front of wind vanes. The vanes maintained the slides normal to the air flow. Moore and Mason fixed the slides across the intake to a suction pump for sampling at low wind speeds. The data from both studies follow the r^{-B} relationship with increasing wind speed associated with a rather consistent pattern of increase in both the number and size of particles.

Most of the presently available experimental and theoretical work on the size distribution of atmospheric aerosols show a continuous size distribution which agrees with the concept of similarity between different size classes and can be described by Junge's size distribution model of $dn/d\log r = Ar^{-B}$.

(c) *Results presented*

This paper presents measured information concerning the significant distinctive features of the atmospheric giant particle size distribution including:

(1) The slope of the size distribution and its variation with changes in location and weather conditions.

(2) The total particle number and mass (calculated) concentration.

(3) The effect of changes in the size distribution slopes on the calculated mass concentration distribution.

The data was obtained during a three months atmospheric sampling program during which 30 samples of giant particles were collected at three different locations. It can be seen from FIG. 1 that published data and data collected during this investigation were comparable within an order of magnitude. As will be discussed later, the slopes reported by Okita are nearly the same as the ones obtained in this study.

2. MEASUREMENT OF ATMOSPHERIC GIANT PARTICLE SIZE DISTRIBUTION

(a) *Method*

The particle samples were collected with a new rotary inertial impactor. NOLL (1970) designed this impactor specifically for collecting a representative sample of atmospheric giant particles in the 5–100 μm radius range. The design of the collector was based on an inertial parameter known as the Stokes number K

$$K = \frac{\rho_p d^2 v_0}{18 \mu L}$$

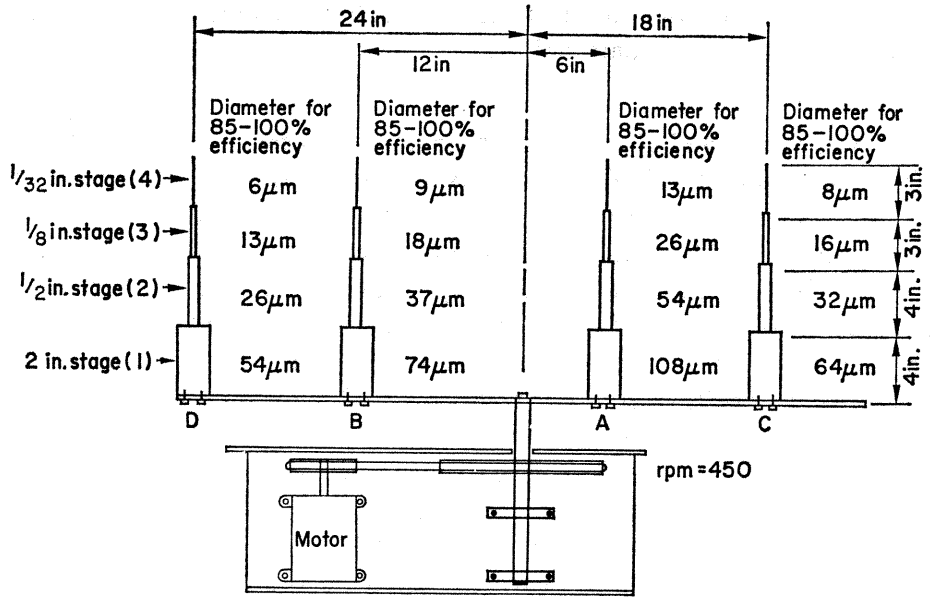

FIG. 2. Atmospheric giant particle inertial impactor.

where ρ_p is the particle density, d the particle diameter, v_0 the undisturbed gas velocity, μ the gas viscosity, and L the width of the rectangular collector. A Stokes number of 10 was selected as the design criteria for the collector stages. This Stokes number corresponds to a particle collection efficiency of between 85 and 100%. For a Stokes number of 10 and a particle density of 2 g cm^{-3}, NOLL (1970) derived the following collector stage design equation for the minimum particle diameter and collected with 85% or greater efficiency

$$d = (HL/v_0)^{1/2}$$

where H is a constant of 0.0162 with cgs units. The 16 stage impactor shown in FIG. 2 with various width rectangular collectors effectively separated the atmospheric aerosol into different size (Stokes number). This size separation greatly reduces the effort required to determine the size distribution by microscopic examination of the collector faces. NOLL and PILAT (1970) compared the theoretical and measured particle concentrations deposited on the collector face and concluded that above a Stokes number of 10 the particle collection efficiency was constant across the face.

Samples of the atmospheric aerosol were collected by exposing the moving rectangular collectors to the outside air for time periods ranging from 15 min to 2 hr. The collector surfaces were coated with vaseline to ensure retention of the impacted particles. To prevent contamination the rectangular collectors were coated in a clean room and stored in air tight plastic tubes before and after sampling. The exposed collectors were returned to the clean room where the collected particles were sized and counted by visual methods using a Zeiss microscope–television camera–TV monitor arrangement. Overhead illumination was used thus allowing the collector face to be viewed directly without any cover glass between the collected particles and the microscope objective lens. The radius intervals in microns for classification of particles were 4–6, 6–9, 9–13, 13–18, 18–22, 22–32, 32–42, 42–53, 53–64, 64–85 and 85–106. At least 50 particles were counted in each size interval to assure a statistically accurate representation of the true concentration. The number of particles counted in each interval was used to calculate the magnitude of $dN/d\log r$ which was then plotted at the center of the radius interval. Each atmospheric giant aerosol size distribution curve has eleven data points.

(b) *Sampling sites*

Sampling was conducted at two sites in Seattle and one site on the Pacific Ocean beach (Ocean City State Park, Copalis, Washington). The primary sampling site was at the Seattle Center. The rotary inertial impactor was located on the fourth floor roof of the Food Circus Building which is in the middle of the park-like six square block Seattle Center. This site was not near any large local sources of giant particles but was exposed to air flow from the Seattle business district (6–12 blocks southwest), the industrial area (3 miles southeast through south), and the Puget Sound (1 mile southwest through northwest). Twenty four samples were collected at the Seattle Center site in order to characterize the size distribution under various meteorological conditions. At least one sample was collected each day for a three week period except during periods of steady rain. During a day of relatively high air pollutant concentrations (March 26, 1969) four samples were taken.

At the second sampling site in Seattle, located on the University of Washington campus (about 4 miles northeast of the Seattle Center), three samples were collected.

The rotary inertial impactor was mounted on a 3 foot high platform on the third floor roof of More Hall (Civil Engineering Department Building). The University power plant and its 250 ft stack is located about 100 yd northeast of this site.

The third sampling site was at Ocean City State Park, Copalis, Washington. Three samples were collected here to determine the influence of the sea salt aerosol on the atmospheric giant particle size distribution. The rotary inertial impactor was located at an elevation of 4 ft above the ground (on a large piece of driftwood) and from 50 to 200 yd from the edge of the Pacific Ocean.

(c) *Data recorded*

In addition to the atmospheric giant particle samples, meteorological data were obtained during each particle sampling period. The recorded meteorological data included prevailing visibility, cloud heights, amount of cloud cover, wind speed and direction, temperature, and relative humidity. Continuous readings of the atmospheric light scattering coefficient, measured with the Charlson–Ahlquist integrating nephelometer, were available at the Seattle Center.

(d) *Approaches for presenting size distribution data*

In general the size distribution data of atmospheric aerosols has been graphically presented in two forms, the number/log radius distribution ($dN/d\log r$ vs. r) used by Junge and the number/radius distribution reported by FRIEDLANDER and PACERI (1965), CLARK and WHITBY (1967), and TAKAHASI and KASAHARA (1968). The relationship between the two distributions is shown below:

$$\frac{dN}{dr} = \frac{1}{r}\frac{dN}{d\log r} = n(r) = Ar^{-B-1},$$

$$\frac{dN}{d\log r} = Ar^{-B}.$$

The data reported in this study are presented as $dN/d\log r$ distributions.

3. DISCUSSION OF RESULTS

(a) *General features of the size distributions*

FIGURE 3 presents the average size distribution for the data collected at each sampling site and shows the following:

(1) The size distribution of giant particles was continuous at all three locations.

(2) The average slope of the size distributions, B, at each site was similar. For the range 5–25 μm it varied only between 2.3 and 3.4 while the average slope in the 40–100 μm range varied only between 5.7 and 6.7.

(3) A transition zone or break in the size distribution curves occurred between 25 and 40 μm radius at all three locations.

The total particle concentration in the range 5–100 μm averaged 2.6×10^{-2} particles cm^{-3} at the Seattle Center, 1.8×10^{-2} particles cm^{-3} at the University of Washington site, and 2.3×10^{-2} particles cm^{-3} at the ocean shore. The calculated total weight of particles (based on spherical particles with a density of 1 g cm^{-3}) between 5 and 100 μm was 224 $\mu g\ m^{-3}$ at the Seattle Center, 125 $\mu g\ m^{-3}$ at the University of Washington, and 77 $\mu g\ m^{-3}$ at the ocean.

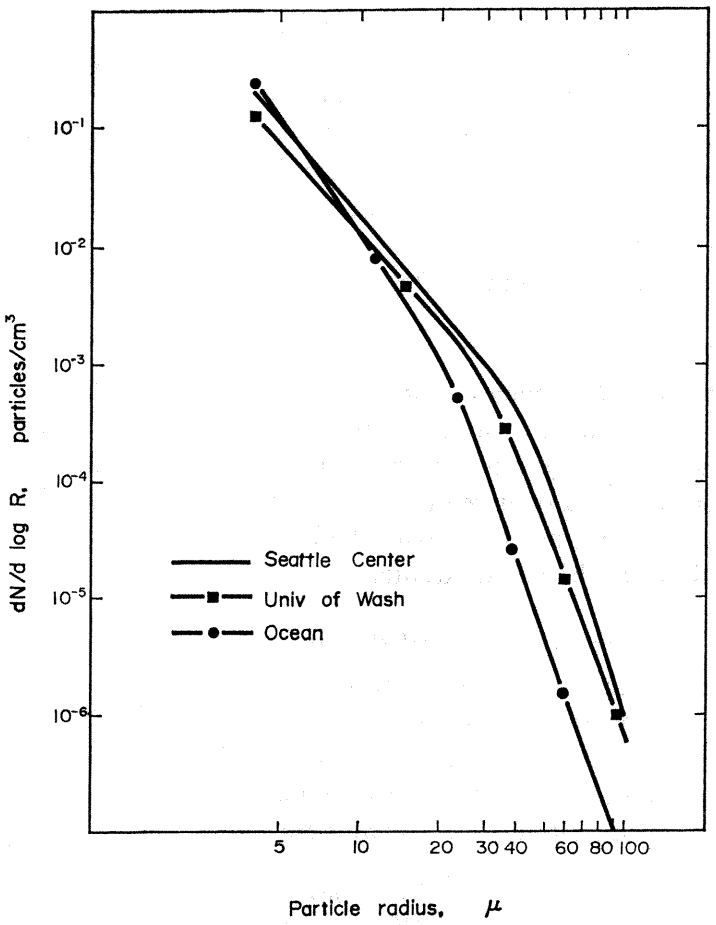

FIG. 3. Atmospheric giant aerosol size distribution at three locations in Washington State.

TABLE 1 provides information on the individual samples collected in this investigation. Columns 1 and 2 contain the code number, and date and hours of sampling, respectively. In column 3 the total concentration of particles between 5 and 100 μm is given. Column 4 shows the calculated total mass of material between 5 and 100 μm in μg m^{-3}. The slope of the distribution between 5 and 25 μm radius and between 40 and 100 μm radius are given in columns 5 and 6 while column 7 provides the size range over which the change in slope occurred. Column 8 contains the average scattering coefficient for the sampling period (AHLQUIST and CHARLSON, 1967). The remaining columns contain pertinent weather information which was collected for each sampling period.

This table shows that the total number of particles in the size range 5–100 varied between 1×10^{-2} and 6.4×10^{-2} particles cm^{-3} while the calculated weight varied over a wide range between 49 and 838 μg m^{-3}. The slope of the particle size distribution, B, in the 5–25 μm range varied from 1.75 to 3.5 with an average value of 2.3. The slope of the particle distribution between 40 and 100 μm varied from 5.0 to 10.0 and averaged 6.7. Although the larger particle range had much more variation in slope, 18 of the 30 samples had slopes between 6 and 7.

TABLE 1 also shows that samples were collected at the Seattle Center with winds from the North, East, South, and West as well as from many other directions. The

TABLE 1. SUMMARY OF GIANT PARTICLE SIZE DISTRIBUTION DATA (1969)

Code no.	Date time	No. cm^{-3} Total $\times 10^{-2}$	$\mu g\ m^{-3}$ Total	Slope (B) 5–25 μm	Slope (B) 40–100 μm	Trans. zone μm	b_{scat} (10^{-4} m^{-1})	Vis. (miles)	R.H. (%)	Wind Dir.	Wind Speed m.p.h.
Seattle Center											
1	14 Mar. 1438–1510	1.7	307	−1.75	−5.0	35–45	1.9	10	48	S	6
2	15 Mar. 1027–1110	1.2	100	−2.25	−7.25	30–40	1.3	15	47	SSW	10+25
3	17 Mar. 1139–1215	2.4	140	−2.75	−7.0	35–45	0.8	15	75	S	15
4	18 Mar. 0906–0951	2.6	185	−2.0	−6.0	25–35	2.5	30	86	S	4
5	19 Mar. 1004–1046	1.7	181	−1.8	−6.0	25–35	0.8	30	72	S	7
6	20 Mar. 0922–1003	2.6	150	−2.5	−8.0	25–35	1.5	10	72	NNE	10
7	21 Mar. 0931–1012	2.9	188	−2.5	−6.0	20–30	2.7	3	71	W	3
8	21 Mar. 1529–1614	1.8	197	−2.0	−6.5	30–40	0.6	30	29	NNW	12
9	23 Mar. 1314–1407	1.0	98	−2.25	−7.0	35–45	0.8	35	30	NNW	7
10	24 Mar. 1140–1233	2.1	136	−2.75	−6.0	30–40	0.9	40	41	NNW	9
11	25 Mar. 1422–1520	2.7	227	−2.0	−7.0	25–35	1.7	20	29	NW	10
12	26 Mar. 0918–0935	5.5	838	−2.0	−6.0	50–60	6.6	3	63	SW	5
13	26 Mar. 1113-1145	1.9	153	−2.5	−8.0	30–40	1.7	15	47	WSW	5
14	26 Mar. 1343–1423	2.7	194	−2.75	−7.0	35–45	1.8	20	33	W	5
15	26 Mar. 1935–1955	6.4	437	−2.25	−8.0	30–40	4.2	7	44	E	3
16	27 Mar. 1009–1024	1.3	127	−2.75	−5.5	35–45	1.7	10	67	SW	8
17	28 Mar. 0910–0928	3.2	188	−2.5	−10.0	25–35	4.5	2	67	NE	7
18	28 Mar. 1512–1607	3.0	211	−2.0	−9.0	25–35	2.8	7	61	W	5
19	29 Mar. 0847–0930	3.6	213	−2.75	−6.0	25–35	3.5	3	75	SW	3
20	29 Mar. 1650–1732	1.0	195	−1.75	−6.5	20–40	2.1	10	56	SW	7
21	30 Mar. 0905–1007	3.7	230	−2.75	−7.5	30–40	3.4	5	62	SW	4
22	31 Mar. 0945–1000	1.7	360	−2.5	−6.0	20–40	0.6	25	—	S	12+25
23	2 Apr. 1025–1040	2.0	187	−2.25	−8.0	35–45	1.7	20	77	S	10
24	3 April. 0922–0942	2.8	140	−3.0	−5.5	35–45	0.8	50	—	SSE	10
Ocean											
25	14 Apr. 1619–1724	1.4	49	−3.3	−6.5	20–30	1.0	—	—	SW	8
26	15 Apr. 1023–1127	3.2	102	−3.4	−6.5	20–30	1.0	—	72	SSW	9

TABLE 1 (*cont.*)

Code no.	Date time	No. cm^{-3} Total $\times 10^{-2}$	$\mu g\ m^{-3}$ Total	Slope (*B*) 5–25 μm	Slope (*B*) 40–100 μm	Trans. zone μm	b_{scat} (10^{-4} m^{-1})	Vis. (miles)	R.H. (%)	Wind Dir.	Wind Speed m.p.h.
Ocean (cont.)											
27	15 Apr. 1454–1627	2.3	80	−3.5	−7.0	25–35	1.0	—	70	SW	6
Univ. of Washington											
28	15 Nov. 1968 1021–1241	1.4	80	−3.0	−6.5	35–45	—	10	40	SE	5
29	12 Mar. 1020–1054	2.0	147	−2.1	−6.0	20–30	—	4	56	SE	3
30	13 Mar. 0923–1061	2.1	154	−2.6	−5.5	20–30	—	4	58	SE	3

wind speed for different sampling periods varied from 3 to 25 m.p.h. Although not shown in this table, samples were collected under many different weather conditions including before and after periods of steady rain, and when there were rain showers near the station. Samples were collected under various levels of air pollution as indicated by variations in the prevailing visibility (2–50 miles) and scattering coefficient measurements (0.6–6.6 $\times$ 10^{-4} m^{-1}).

TABLE 2 shows the correlation coefficients between the various parameters listed in TABLE 1 for the samples collected at the Seattle Center. The purpose of this table is to provide specific information on the inter-relationship of the variables (wind speed, b_{scat}, number of particles cm^{-3}, size distribution slope, location of transition zone). From this set of correlation coefficients it can be inferred that there was little direct connection between the various parameters. However, b_{scat} showed the highest and most consistent correlation to the other variables with a correlation coefficient of − 0.58 to wind speed, + 0.79 to total number of particles and + 0.69 to calculated total mass of material. The total mass of material had the second best set of correlation coefficients with a + 0.66 to total number of particles and + 0.47 to the location of the transition zone.

TABLE 2. CORRELATION COEFFICIENTS FOR VARIABLES AT SEATTLE CENTER FROM TABLE 1.

	Wind speed	Locat. tran.	b_{scat}	Total (No. cm^{-3})	Total ($\mu g\ m^{-3}$) (calculated)	Slope 5–25	Slope 40–100
Wind speed	1.0	+0.26	−0.58	−0.46	+0.15	+0.06	+0.07
Locat. tran.		1.0	+0.16	+0.10	+0.47	+0.01	−0.32
b_{scat}			1.0	+0.79	+0.69	−0.05	+0.26
Total (No. cm^{-3})				1.0	+0.66	+0.13	+0.23
Total ($\mu g\ m^{-3}$)					1.0	−0.24	−0.11
Slope 5–25						1.0	+0.02
Slope 40–100							1.0

There was some dependence of the total concentration of particles on the wind speed as shown by the — 0.46 correlation coefficient. This was further verified by separating the data into two groups. One with average wind speeds less than 10 m.p.h. and the other with wind speeds equal to or greater than 10 m.p.h. When the size distribution data for each group was averaged together there were about twice as many particles at all sizes in the group with the lower wind speeds.

There was no obvious correlation between the location of the transition zone and the wind direction or speed. This implies that the location of the transition zone was not determined by different source characteristics.

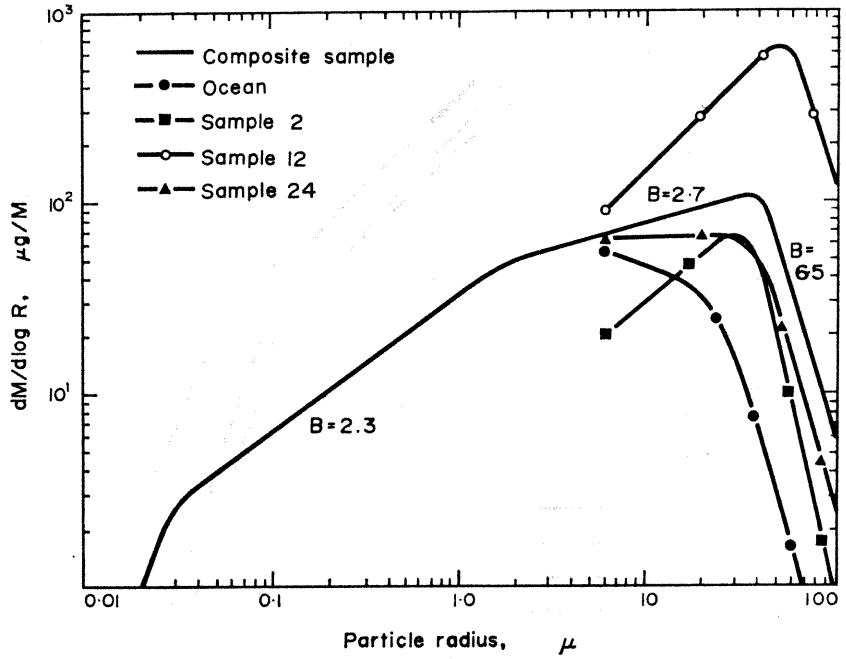

FIG. 4. Calculated weight distribution of five atmospheric giant aerosol samples.

FIGURE 4 shows the calculated mass distribution versus the particle size for some of the distributions in TABLE 1. This figure shows the effect that different slopes (size distribution vs. radius) have on the mass distribution. For a $B = 3$ (sample 24) the curve for the mass distribution is parallel to the log r-axis ($dM/d\log r$ = constant); if B is less than 3 (samples 2 and 12) it means an upward trend and if B is greater than 3 (ocean) a downward trend in the mass distribution vs. radius. The majority of the aerosol mass is centered below 50 μm because of the rapid drop off in the number of particles above this size (shown by the larger slopes). The important results shown by FIG. 4 is that the mass of material can be distributed over the giant particle size range in many different ways depending on the slope of the distribution and the location of the transition zone.

The location of the transition zone is very significant to the mass concentration of samples with a slope of 3 or less because particle sizes near the transition zone contribute greatly to the total weight. This is shown by the fact that the peak of the mass distribution curves are generally located in the 30–50 μm range.

(b) *Variations in giant particle size distribution during high air pollution period*

FIGURE 5 shows four size distributions (12, 13, 14, 15) which were collected on March 26 at the Seattle Center. This day was significant because relatively large amounts of pollution accumulated in the Seattle area due to stable air and low winds. TABLE 1 lists the wind speed and directions, and the time periods during which the four samples were collected.

A land breeze which developed during the night (east 3–5 m.p.h.) carried polluted air from the Seattle area out over Puget Sound. A sea breeze developed near 0730

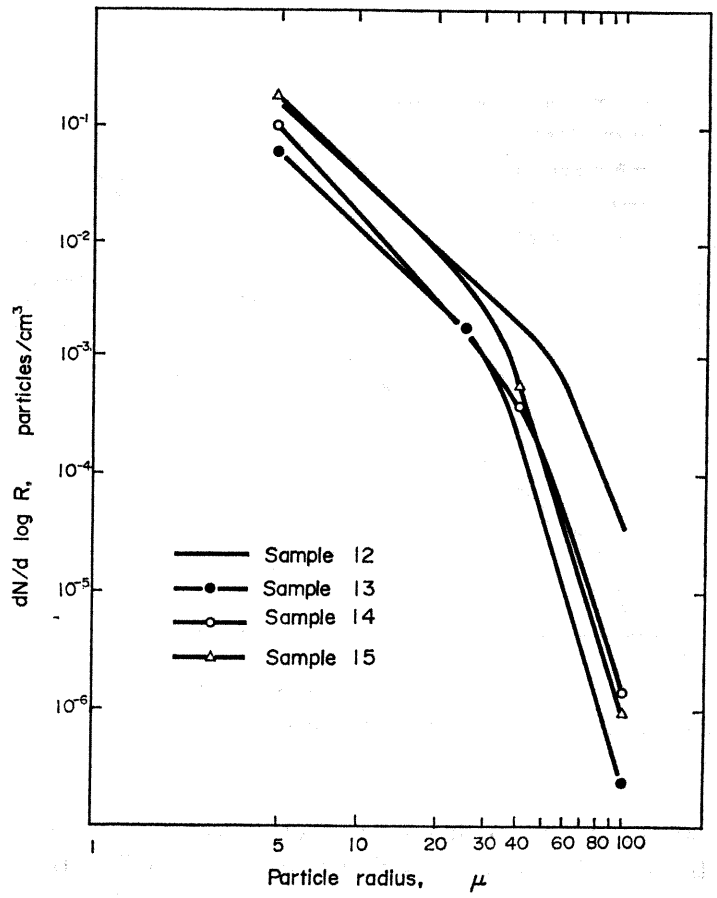

FIG. 5. Atmospheric giant aerosol size distributions obtained on March 26, 1969 at Seattle Center.

(west 5 m.p.h.) and the accumulated material was carried over the sampling site. The polluted cloud was then carried east of the station and was followed by cleaner air off the Sound. Near 1700 the sea breeze at the sampling site was replaced by a land breeze and the cloud of pollution which had moved east of Seattle was again carried over the station.

Two of the four samples (12 and 15) were collected during the morning and evening pollution periods. The other two were obtained between the higher pollution periods when cleaner air from Puget Sound was over the station. TABLE 1 shows that there were nearly 3 times as many giant particles present during the high pollution periods as there were during the intervening sampling periods.

FIGURE 5 shows that the slope of the size distributions were similar for the four samples in the range 5–25 μm (2.0–2.6). The slope above 25 μm varied between 6.0 and 8.5. The transition zones for the two cleaner air samples and the evening sample were near 35 μm while the early morning sample had a transition zone near 55 μm.

The computed mass between 5 and 100 μm for the early morning sample was 838 $\mu g\ m^{-3}$ while the evening sample had a calculated total mass of 437 $\mu g\ m^{-3}$. This

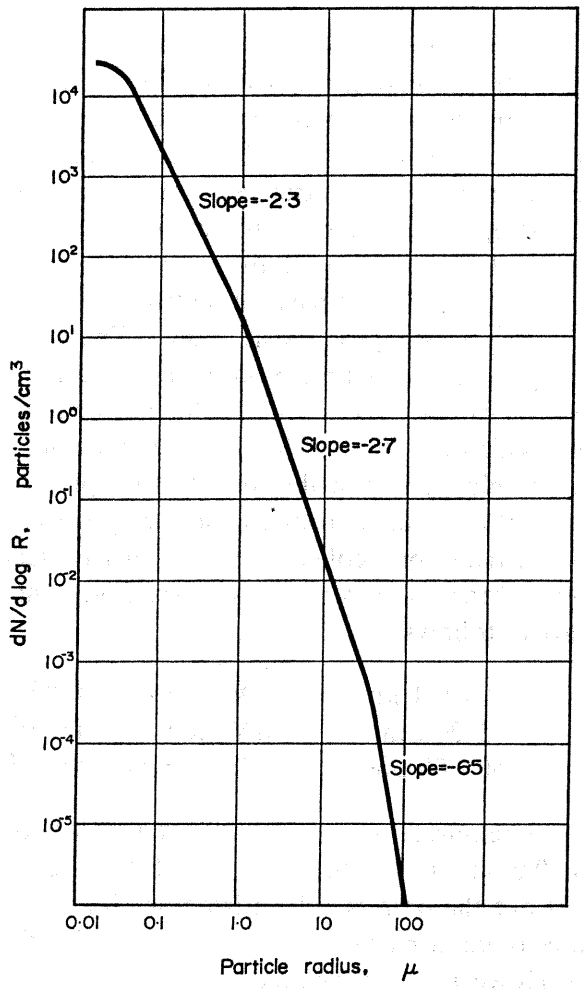

FIG. 6. Complete atmospheric aerosol size distribution resulting from averaged thermal precipitator and rotary impactor data.

was nearly a 50 per cent change in mass. The calculated mass of material in samples 13 and 14 was 127 and 188 $\mu g\ m^{-3}$ respectively and this amounted to about 20 per cent of the mass in the early morning sample.

FIGURE 5 shows that the major change in particle concentration between samples 12 and 15 occurred above 35 μm. This resulted in a significant difference in the particle mass concentration and the particle mass vs. size distribution between these two samples. Sample 12 had 53 per cent of the total mass above 35 μm and 30 per cent above 50 μm while sample 15 had only 13 per cent of the total mass above 35 μm and 5 per cent above 50 μm.

These samples demonstrate the importance of the history of the air being sampled to the particle mass concentration and to its size and mass distribution. It can be assumed that sample 12 had a greater number of particles larger than 35 μm because they had only recently been added to the air mass. Later they settled out during the day so that the aged aerosol which returned in the evening (sample 15) had fewer particles in the 35–100 μm range. This resulted in a large decrease in the total giant particle mass concentration and a change in the mass distribution with size.

(c) *Mass distribution of atmospheric aerosol*

Information on the contribution of giant particles to the total mass of atmospheric aerosol is important to air pollution engineers because most sampling programs for atmospheric aerosol are conducted with high volume sampling instruments which measure the total mass of particulate matter collected on mat filters but provide no size classification. A first approximation of the relative importance of giant particles to the total mass of aerosol is provided here by combining data from this study with previous data on the size distribution of particles between 0.01 and 2 μm. The data was collected in 1966 in Seattle, Washington (NOLL, 1967). The sampling instrument used for the investigation was a thermal precipitator. The precipitator was modified to provide a uniform deposit of particles instead of the uneven deposit which is collected with most instruments which use thermal forces for collection.

FIGURE 6 shows a complete size distribution of atmospheric aerosol from 0.01 to 100 μm obtained by combining data from 14 thermal precipitator samples with the 24 giant particle size distributions collected at the Seattle Center. This composite distribution has three different slopes and two transition zones. The slopes for the different size ranges are as follows:

0.01–1 μm	$dN/d\log r = Ar^{-2.3}$
2–30 μm	$dN/d\log r = Ar^{-2.7}$
50–100 μm	$dN/d\log r = Ar^{-6.5}$

Some adjustment was required in the slopes of the two sets of data to make a continuous distribution (0.01–1 μm change from -2.5 to -2.3 and 2–30 μm change from -2.3 to -2.7) but the data is still satisfactory for making a first estimate of the relative importance of giant particles to the total mass for the atmospheric aerosol from 0.01 to 100 μm. However the combined data is somewhat uncertain as the giant particle measurements were made some 3 yr after the small particle data was obtained.

FIGURE 4 shows the mass distribution vs. particle size for the composite distribution. There is a positive slope to the mass distribution vs. radius line between 0.01 and 30 μm. This gradual increase in the proportion of mass contributed by each size makes the giant particle size range extremely important to the total mass of aerosol. The total calculated mass for the composite distribution was 295 $\mu g\ m^{-3}$ and only 20 per cent of this was located below 1 μm. This compares with a total number of particles equal to $1.4 \times 10^4\ cm^{-3}$ of which 99 per cent were smaller than 1 μm. Thirty-five per cent of the mass was distributed in the 1–10 μm range while 45 per cent was between 10 and 50 μm. There was a negligible amount above 50 μm radius (less than 1 per cent). The mass median diameter for the composite distribution was near 4 μm and the standard geometric deviation was near 6.0.

The total mass of giant particles calculated throughout this paper seem higher than would be expected based on measurements of total weight obtained with such instruments as the high volume sampler. This is probably due to the large inertia of giant particles which prevents their collection with a high degree of efficiency by most sampling instruments (WATSON, 1954; MELAND, 1968). Thus variations in wind speed and direction and the requirement for directional change of the air sample into a shelter or into a tube or duct introduces nonisokinetic sampling conditions which tend to exclude giant particles.

4. SUMMARY

The giant atmospheric particle size distribution measured at three locations in Washington (two in Seattle and one on the Pacific Ocean beach) are similar and are continuous with previous measurements of the 0.01–1 μm radius range of the atmospheric aerosol. The slope of the giant atmospheric aerosol size distribution averages 2.3 in the 5–25 μm radius range and 6.7 in the 40–100 μm radius range. The average location of the transition zone between the two slope ranges was between 30 and 40 μm radius. The location of this transition zone has a substantial effect on the calculated aerosol mass concentration. The giant atmospheric particles contribute a considerable portion to the calculated mass concentration for the complete atmospheric aerosol size distribution (0.01–100 μm radius).

As the giant atmospheric aerosol size distributions presented in this paper were collected at only three locations, more sampling data is needed to accurately describe the possible variations between natural and urban regions. However, it appears that the transition zone between 30 and 50 μm radius is a general feature of atmospheric aerosols.

Acknowledgements—This research was supported by U.S. PHS National Air Pollution Control Administration Special Fellowship No. 1F3 AP 38, 939-01 and National Air Pollution Control Administration Training Grant AP-29. The discussions with and assistance of Dr R. J. CHARLSON and Dr A. T. ROSSANO are gratefully acknowledged.

REFERENCES

AHLQUIST N. C. and CHARLSON R. J. (1967) A new instrument for evaluating the visual quality of air. *J. Air Pollut. Control Ass.* **17**, 467–469.

CLARK W. E. and WHITBY K. T. (1967) Concentration and size distribution measurements of atmospheric aerosols and a test of the theory of self-preserving size distribution. *J. atmos. Sci.* **24**, 677–687.

FRIEDLANDER S. K. and PACERI R. E. (1965) Measurements of the particle size distribution of the atmospheric aerosol: I. Introduction and experimental methods. *J. atmos. Sci.* **22**, 571–576.

FRIEDLANDER S. K. and WANG C. S. (1966) The self-preserving particle size distribution for coagulation by Brownian Motion. *J. Colloid Interface Sci.* **22**, 126–132.

JAENICKE R. and JUNGE C. (1967) Studien zur Oberen Grensgrosse des Naturlichen Aerosoles. *Beitr. Phys. Atmos.* **40**, 129–143.

JOHNSON R. E., ROSSANO A. T. and SYLVESTER R. O. (1966) Dustfall as a source of water quality impairment. *J. Sanit. Engng Div. Am. Soc. civ. Engrs* **92** (SAI), 245–256.

JUNGE C. E. (1955) The size distribution and aging of natural aerosol as determined from electrical and optical data on the atmosphere. *J. Met.* **12**, 13–25.

MELAND B. R. (1968) A comparative study of particulate loading in plumes using multiple sampling devices. *J. Air Pollut. Control Ass.* **18**, 529–533.

MOORE D. J. and MASON M. J. (1954) The concentration, size distribution and production rate of large salt nuclei over the ocean. *Q. J. Roy. Met. Soc.* **80**, 583–590.

NOLL K. E. (1967) A procedure for measuring the size distribution of atmospheric aerosol. *Trend Engng* **19**, 21–27.

NOLL K. E. (1970) A rotary inertial impactor for sampling giant particles in the atmosphere. *Atmospheric Environment* **4,** 9–20.

NOLL K. E. and PILAT M. J. (1970) Inertial impaction of particles upon rectangular bodies. *J. Colloid Interface Sci.* **33,** 197–207.

OKITA (1955) *J. Met. Soc. Japan.* **2,** 291.

PILAT M. J. (1968) Application of gas-aerosol adsorption data to the selection of air quality standards. *J. Air Pollut. Control. Ass.* **18,** 751–753.

TAKAHASHI K. and KASAHARA M. (1968) A theoretical study of the equilibrium particle size distribution of aerosols. *Atmospheric Environment* **2,** 441–453.

TWOMEY S. (1954) The composition of hygroscopic particles in the atmosphere. *J. Met.* **11,** 334–337

WATSON H. H. (1954) Errors due to anisokinetic sampling of aerosols. *Am. Ind. Hyg. Ass. Quart.* **15,** 21–32.

WOODCOCK A. H. and GIFFORD M. M. (1949) Sampling atmospheric sea-salt nuclei over the ocean. *J. mar. Res.* **8,** 177–197.

WOODCOCK A. H. (1952) Atmospheric salt particles and raindrops. *J. Met.* **9,** 200–212.

WOODCOCK A. H. (1953) Salt nuclei in marine air as a function of altitude and wind force. *J. Met.* **10,** 362–371.